Supporting Information for

Inducing Single-Molecule Magnet Behavior with a Single Metal Center Derived from Peripheral Ligand Modifications

Titel Jurca, Ahmed Farghal, Po-Heng Lin, Ilia Korobkov, Muralee Murugesu and Darrin S. Richeson

Centre for Catalysis Research and Innovation and Department of Chemistry, University of Ottawa, Ottawa, Ontario, K1N 6N5

Experimental Details

General:

Reactions were performed in a glovebox under a nitrogen atmosphere, with the exception of ligand synthesis, which was performed using standard Schlenk techniques under a N_2 atmosphere. All solvents were sparged with nitrogen and then dried by passage through a column of activated alumina using an apparatus purchased from Anhydrous Engineering. Cobalt(II) thiocyanate was purchased from Strem Chemicals and used as received. All other chemicals were purchased from Aldrich and used without further purification. Compounds **1** and **2** were synthesized according to literature procedures.[1] Elemental analyses for **3**, and **4** were performed by Midwest Microlab LLC, Indianapolis IN.

Magnetic Meaurements:

The magnetic susceptibility measurements were obtained using a Quantum Design SQUID magnetometer MPMS-XL7 operating between 1.8 and 300 K for dc-applied fields ranging from –7 to 7 T. Direct current (dc) susceptibility measurements were performed on freshly filtered crushed polycrystalline sample of **3** (19.9 mg) and **4** (10.1 mg), wrapped in a polyethylenemembrane. Sample preparation for compound **3** was carried out rapidly in order to avoid any solvent loss. Alternating current (ac) susceptibility measurements were carried out under an oscillating ac field of 3 Oe and ac frequencies ranging from 1 to 1500 Hz. In order to eliminate intermolecular interactions in **4**, crystals (18.2mg) were fully dissolved in THF in a sealed tube and dc and ac susceptibility measurements were carried out on the resulting frozen solution below 50 K. A diamagnetic correction was applied for the sample holder and Pascal constants were used for the diamagnetic correction of the sample. The magnetization data were collected at 100 K to check for ferromagnetic impurities that were absent in all samples.

Synthesis:

[Co[2,6-Bis{1-[(2,6-diisopropylphenyl)imino]ethyl}pyridine](NCS)$_2$](CH$_2$Cl$_2$] (**3**):
$Co(SCN)_2$ powder (0.099 g, 0.57 mmol) was added to a clear yellow solution of **1** (0.300 mg, 0.623 mmol) in 5 mL of toluene. The reaction mixture was sealed and allowed to stir for 6 h. A color change from translucent yellow to translucent green was observed. The solution was then cooled to -20^{o}C for 48 h, to produce a light green precipitate. The reaction mixture was filtered; the solid was washed with 3 x 5 mL hexanes, and dried under vacuum. A light green powder of **3** was isolated in 97% yield. Crystals suitable for X-ray analysis were grown by slow vapor diffusion of hexanes into a moderately saturated solution of **3** in CH_2Cl_2 at -20^{o}C for several days. Elemental analysis performed on crystals grown from a saturated solution of CH_2Cl_2 in hexanes $[C_{35}H_{43}CoN_5S_2]_3[CH_2Cl_2]$: Calcd. C 61.94, H 6.42, N 10.22, Found C 62.28 H 6.40, N 10.25.

---

[1] T. Jurca, K. Dawson, I. Mallov, T. Burchell, G. P. A. Yap, and D. S. Richeson *Dalton Trans*, 2010, ***39***, 1266; R.-Q. Fan, D.-S. Zhu, Y. Mu, G.-H. Li, Y.-L. Yang, Q. Su, and S.-H. Feng *Eur. J. Inorg. Chem.* **2004**, 4891.

[Co[2,6-Bis{1-[(2,6-diisopropylphenyl)imino]benzyl}pyridine](NCS)$_2$], (**4**):
$Co(NCS)_2$ powder (0.056 mg, 0.32 mmol) was added to a clear yellow solution of **2** (0.200 mg, 0.330 mmol) in 5 mL of toluene. The reaction mixture was sealed and allowed to stir for 6 h. A color change from translucent yellow to translucent brown was observed. The solution was then cooled to -20^{o}C for 48 h, to produce a light brown precipitate. The reaction mixture was filtered, the solid was washed with 3 x 5 mL hexanes, and dried under vacuum. A light brown powder of **4** was isolated in 95% yield. Crystals suitable for X-ray analysis were grown by slow vapor diffusion of hexanes into a saturated solution of **4** in THF at -20^{o}C for several days. Elemental analysis for $C_{45}H_{47}CoN_5S_2$: Calcd. C 69.21, H 6.07, N 8.97, Found C 68.95, H 5.99, N 8.88.

Computational Model

The distortion of the ligand environment around the Co center, as discussed in the manuscript, were modeled using DFT computations that were carried out using the Gaussian 09 program suite and employing the B3LYP functional and DGDZVP basis set. The model compound $Co(NH_3)_5^{2+}$ was examined using two different geometric ligand arrays; a square pyramidal ligand geometry with the Co center in the basal plane("ideal") and a geometry with the Co center raised by 0.5 Å out of the basal plane ("elevated"). The metal ligand bond lengths (Co-NH_3 = 1.86 Å) were kept constant for both "ideal" and "elevated" geometries.

The following relative orbital arrangements were obtained:

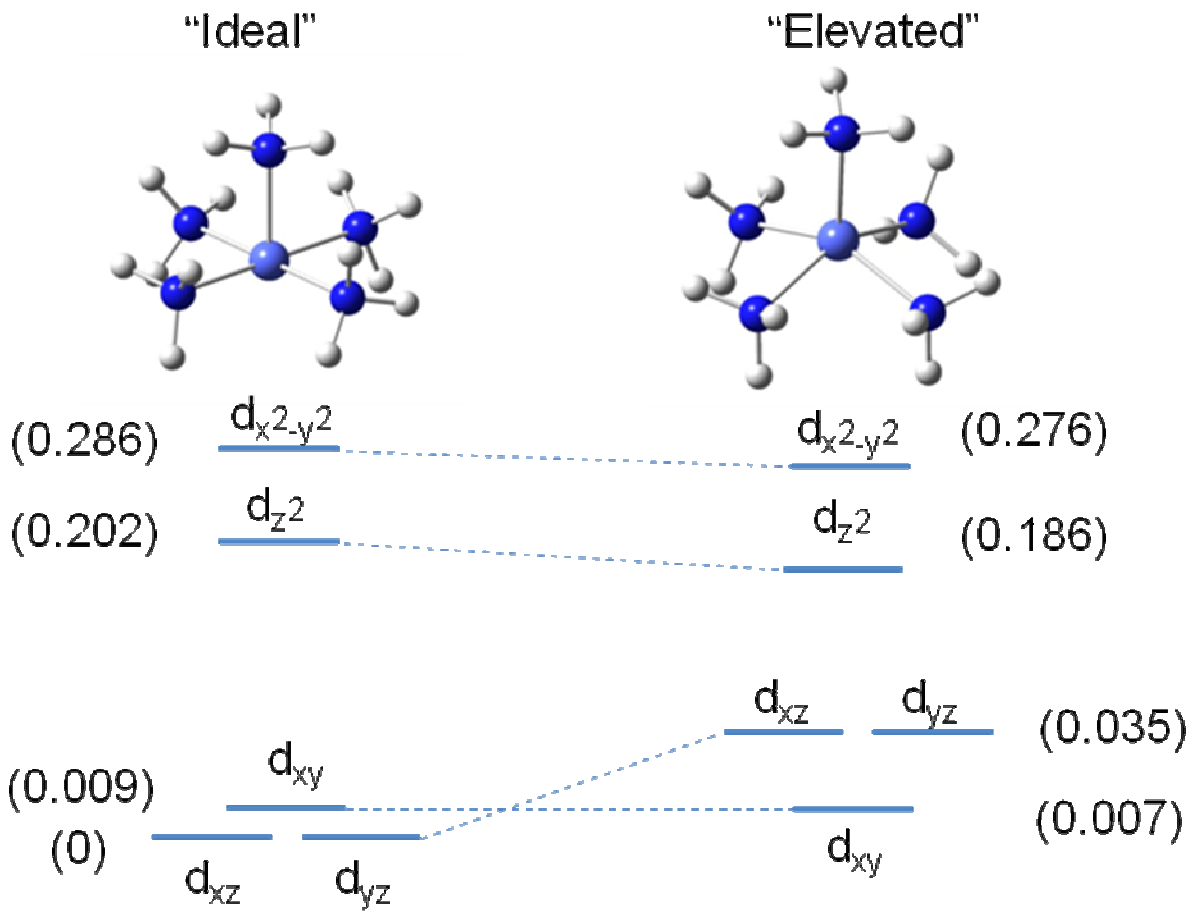

The orbital energies are in atomic units and have been listed relative to the lowest energy orbital having a zero value. These results were used for the model proposed in the manuscript text and represented by Scheme 2.

Figure S1. UV-Vis spectrum Co compounds **3** and **4** obtained in dichloromethane (DCM) and THF. The THF recorded spectra of compound **3** is shown in red and compound **4** in blue. The DCM recorded spectrum of **3** is shown in green and compound **4** in purple. The maximum wavenumber value was determined by background THF absorbance (shown below). The inset provides a magnification of the low energy bands.

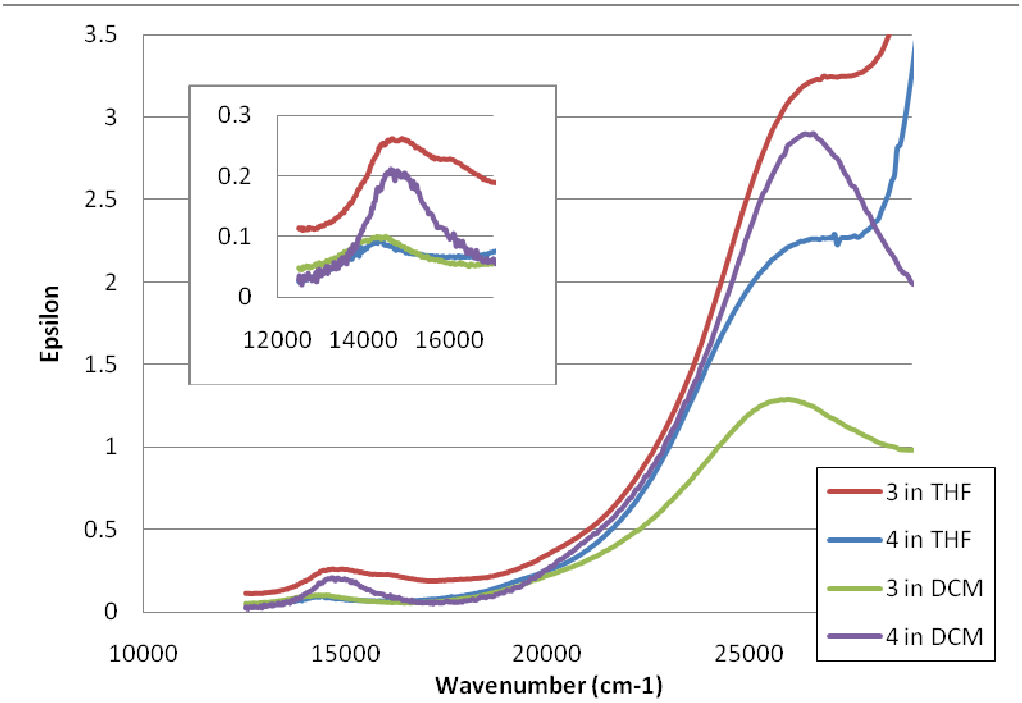

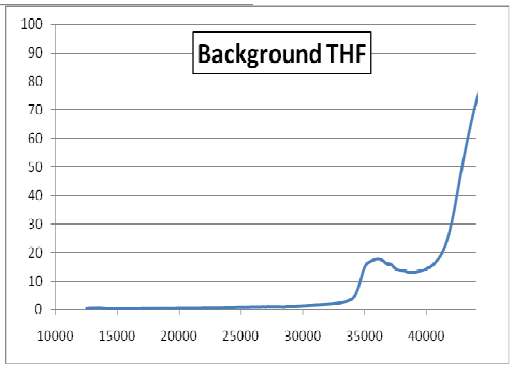

Table S1. Data for compounds **3** and **4**.

ν_{max} (cm^{-1}) (ε_{molar})			
3 in THF	**4 in THF**	**3 in DCM**	**4 in DCM**
26800 (3.25)	27100 (2.3)	25900 (3.9)	26600(2.9)
14700 (0.26)	14400 (0.10)	14500 (0.12)	14600(0.21)

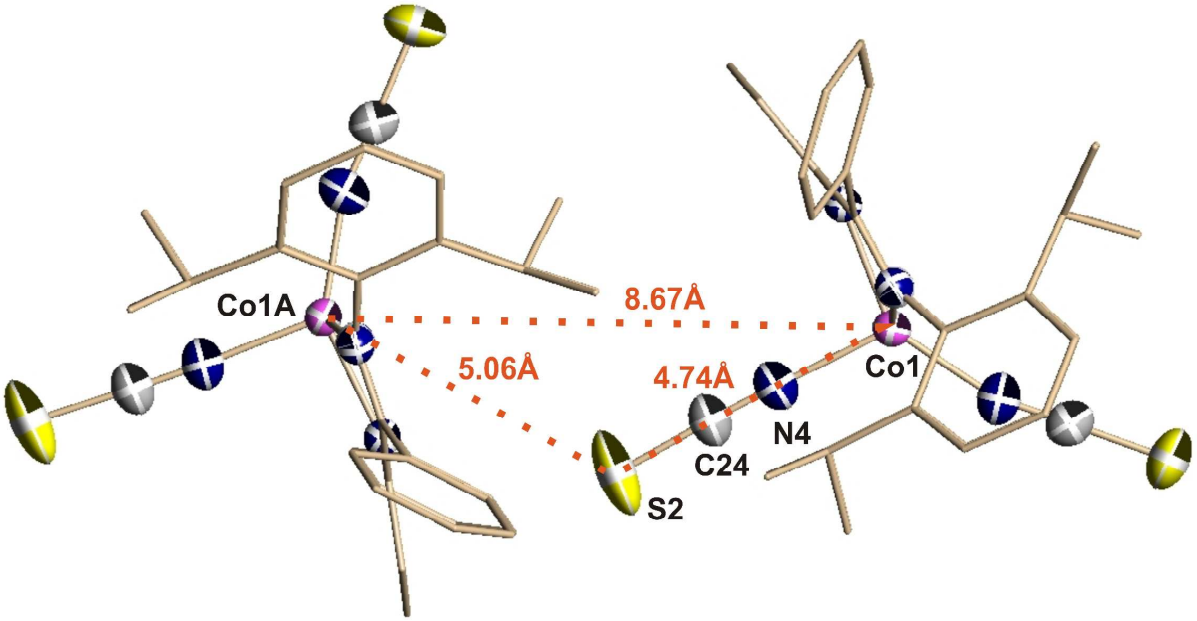

Figure S2. The intermolecular interactions for compound **4** as discussed in the manuscript.

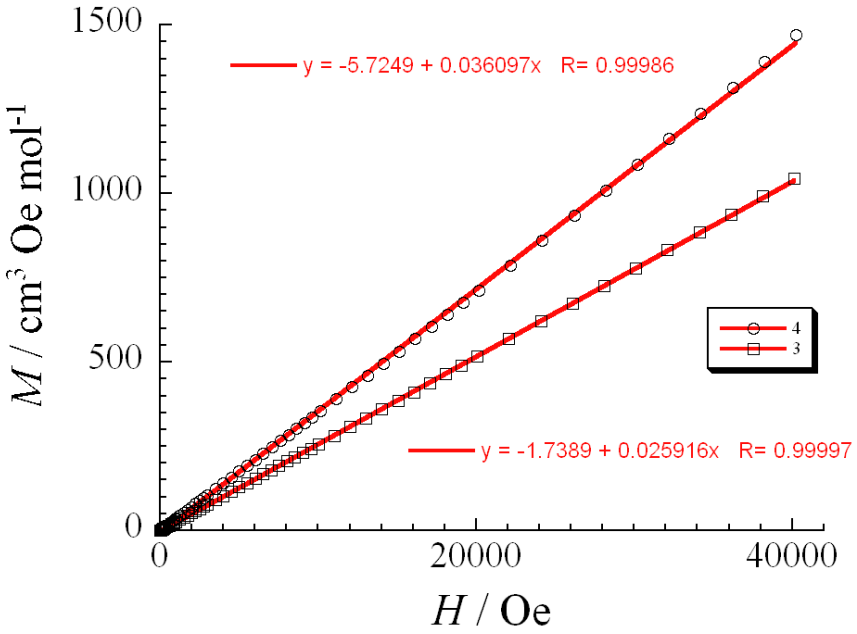

Figure S3. The field-dependent magnetization measured at 100 K for **3** and **4** in order to detect the presence of any bulk ferromagnetic impurities.

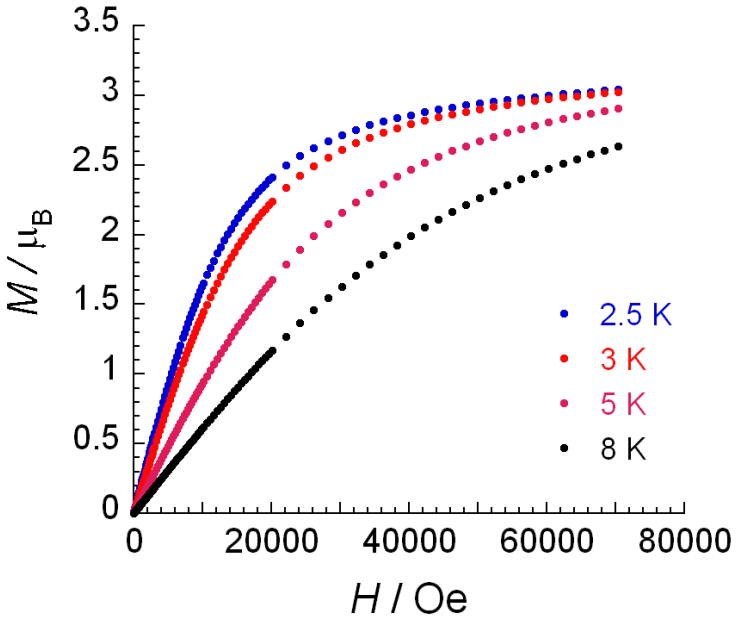

Figure S4. Field dependence of the magnetization, *M*, at 2.5, 3, 5 and 8 K for **3**

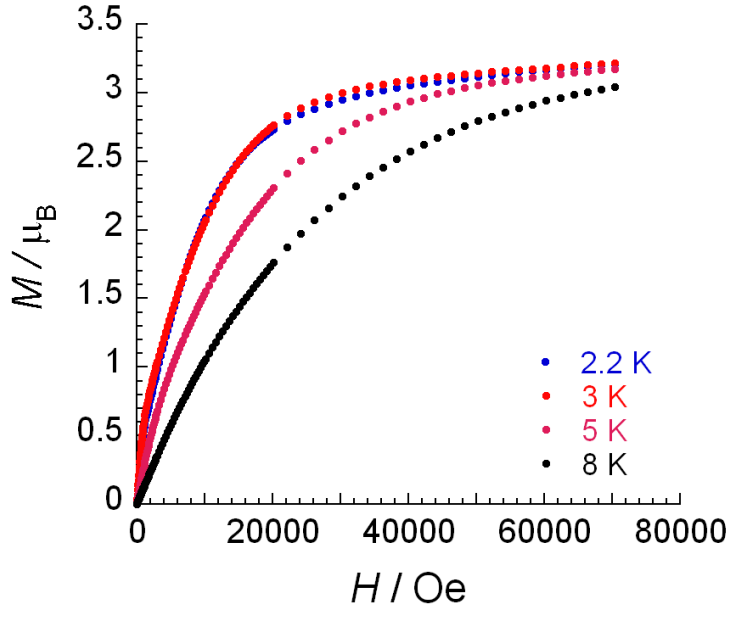

Figure S5. Field dependence of the magnetization, *M*, at 2.2, 3, 5 and 8 K for **4**

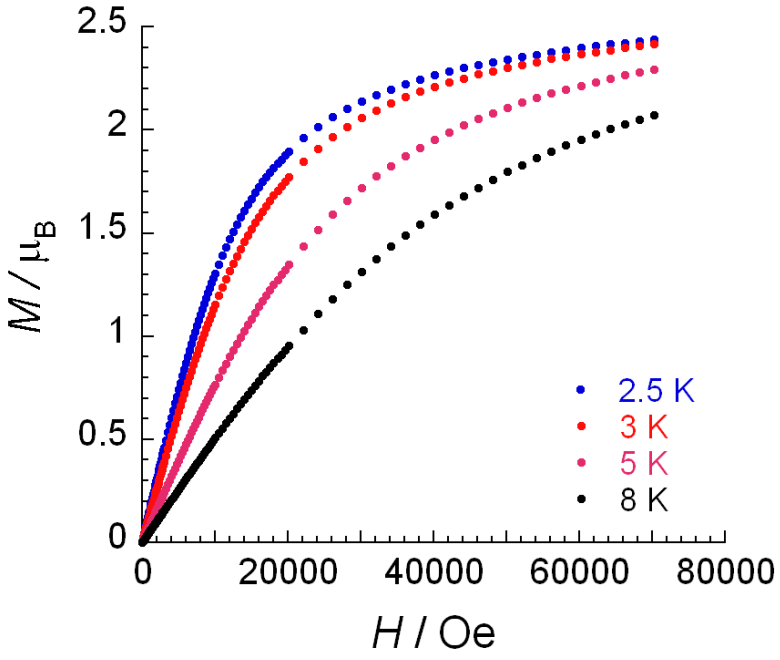

Figure S6. Field dependence of the magnetization, *M*, at 2.5, 3, 5 and 8 K for **4-S**

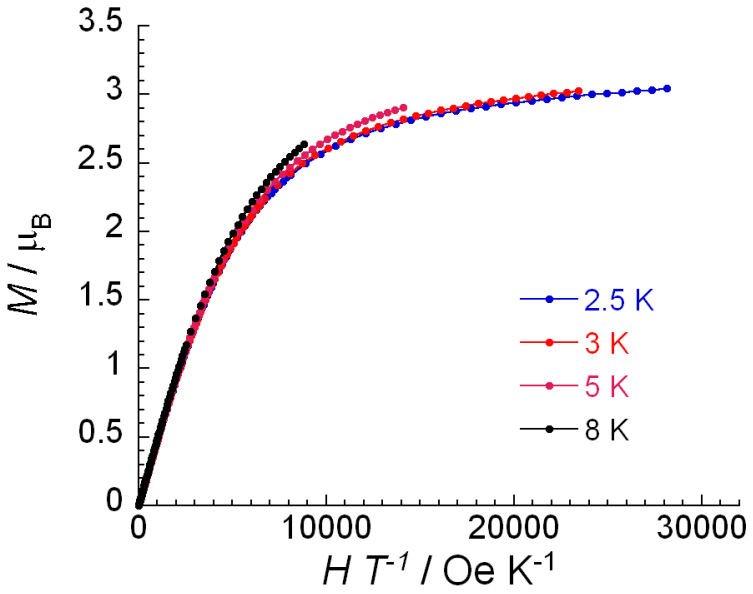

Figure S7. ***M vs. H/T*** **plots at 2.5, 3, 5 and 8 K for 3.**

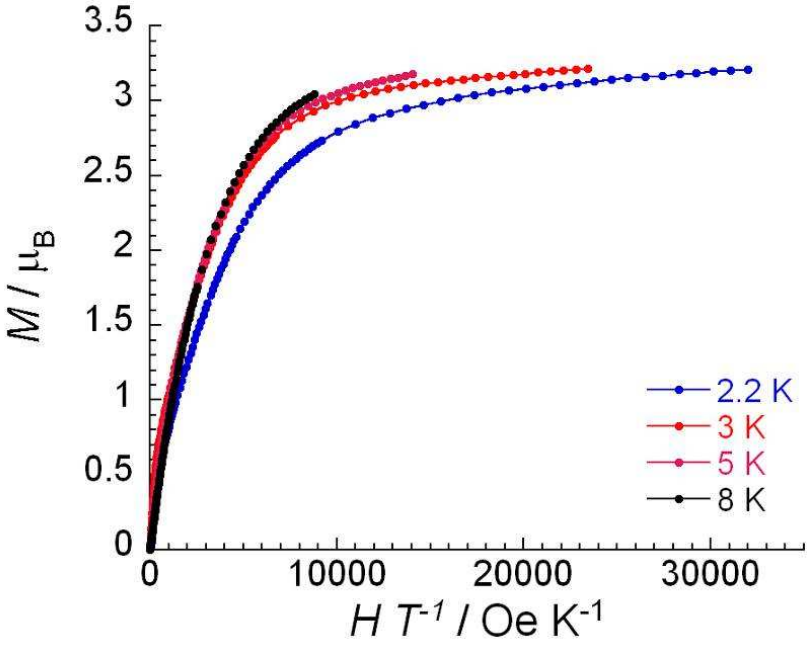

Figure S8. ***M vs. H/T*** **plots at 2.2, 3, 5 and 8 K for 4.**

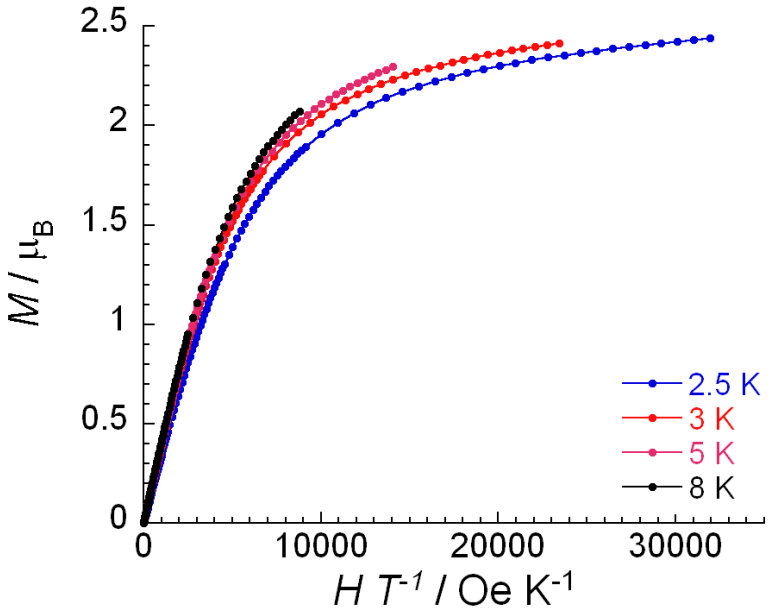

Figure S9. ***M vs. H/T*** **plots at 2.5, 3, 5 and 8 K for 4-S.**

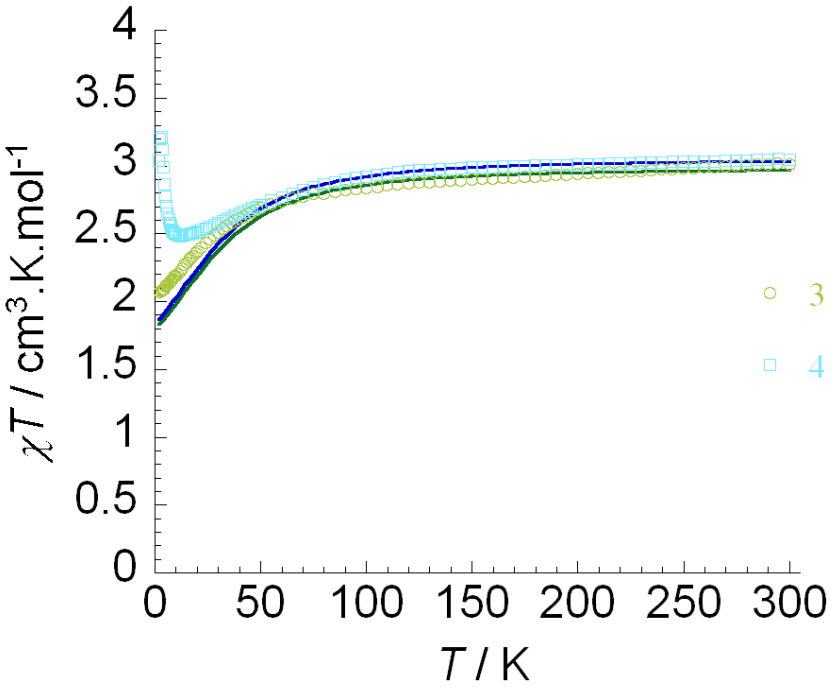

Figure S10. Temperature dependence of the χT product at 1000 Oe for complexes 3 and 4 (with χ being the molar susceptibility per mononuclear complex defined as M/H). Pale green and blue data points are for solid samples of 3 and 4, respectively. Solid lines represent the obtained fits using following equation, which includes axial zero-field splitting parameter.

$$\chi T = \frac{Ng^2\beta^2}{k}\frac{1+9e^{-2x}}{4(1+e^{-2x})} + \frac{2Ng^2\beta^2}{k}\frac{4+\left(\frac{3}{x}\right)(1-e^{-2x})}{4(1+e^{-2x})}$$

where x=D/kT

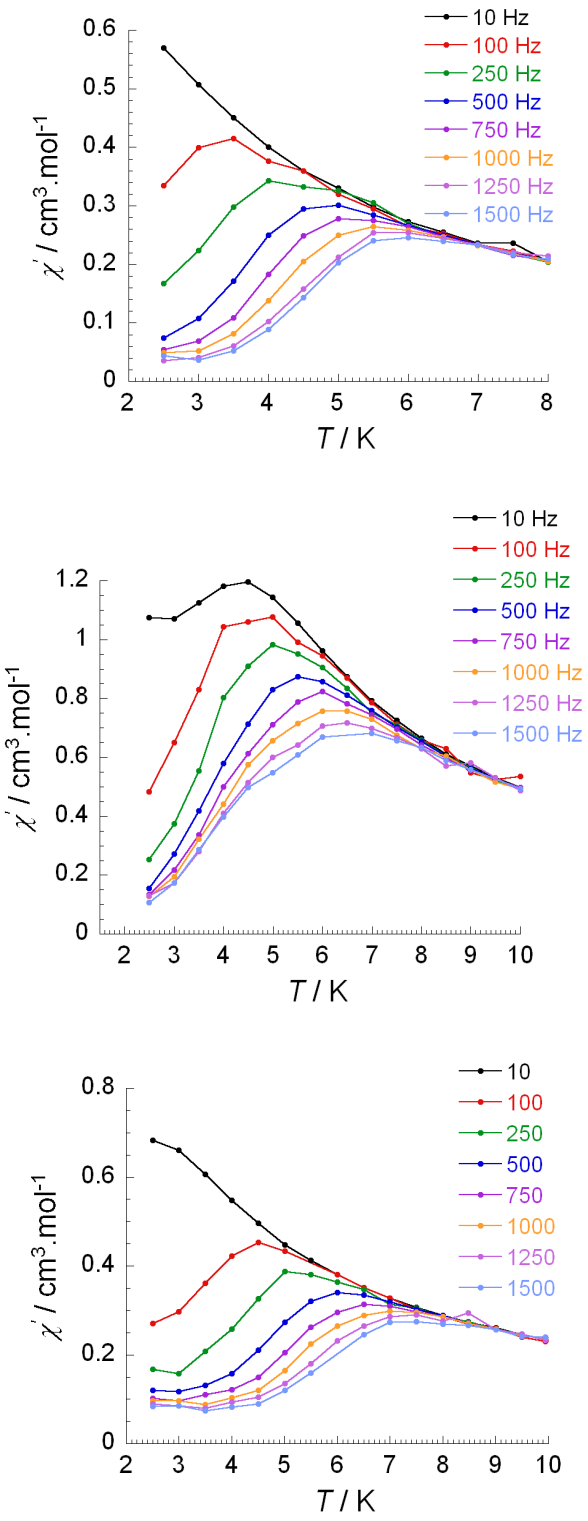

Figure S11: Temperature dependence of the in-phase χ' ac susceptibility signals **3** (top) and **4** (middle: solid state, bottom: solution), collected over the temperature range 2.5-10 K at under an applied dc field of 2000 Oe.

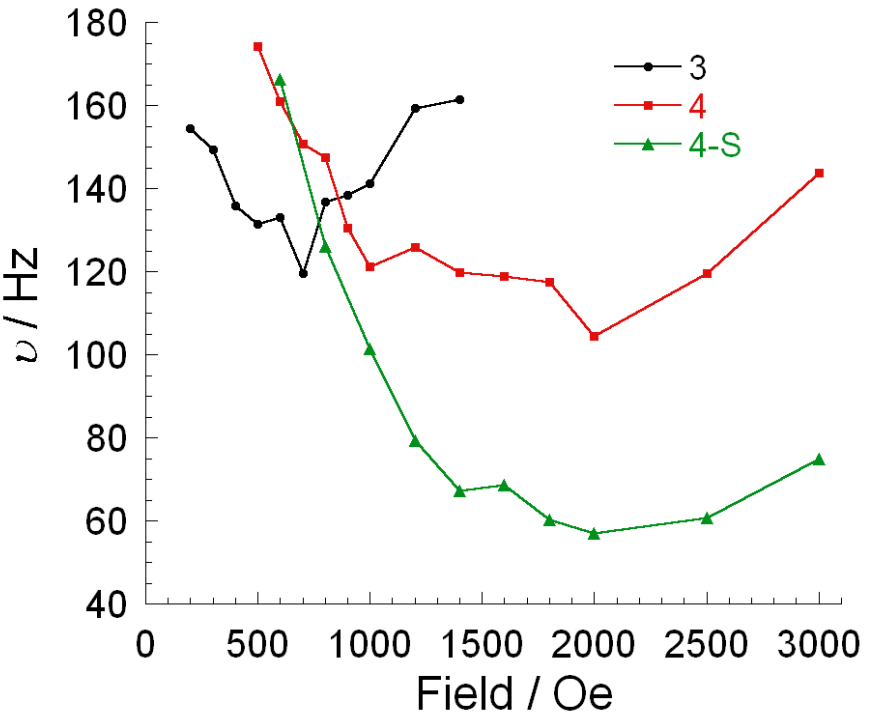

Figure S12. Field dependence of the characteristic frequency (maximum of χ'') as a function of the applied dc field for 3 (black circle), 4 (red square) and 4-S (green triangles) at 3K. Line is guide for the eyes.

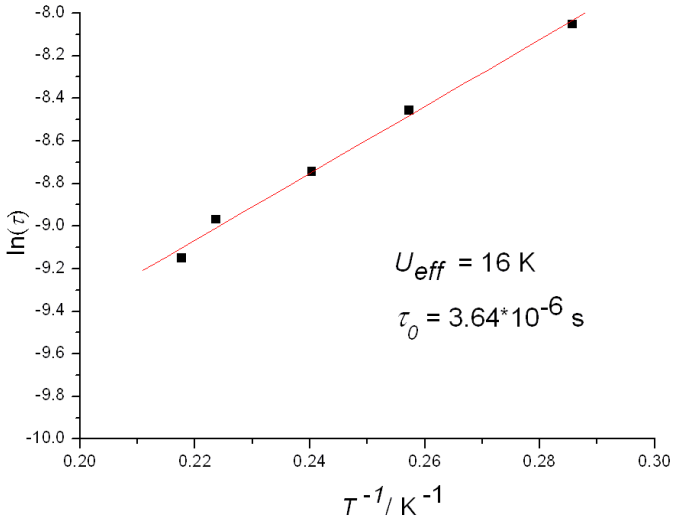

Figure S13. Relaxation time of the magnetization ln(τ) *vs*. T^{-1} (Arrhenius Plot using ac data) of 3. The solid line corresponds to the fit.

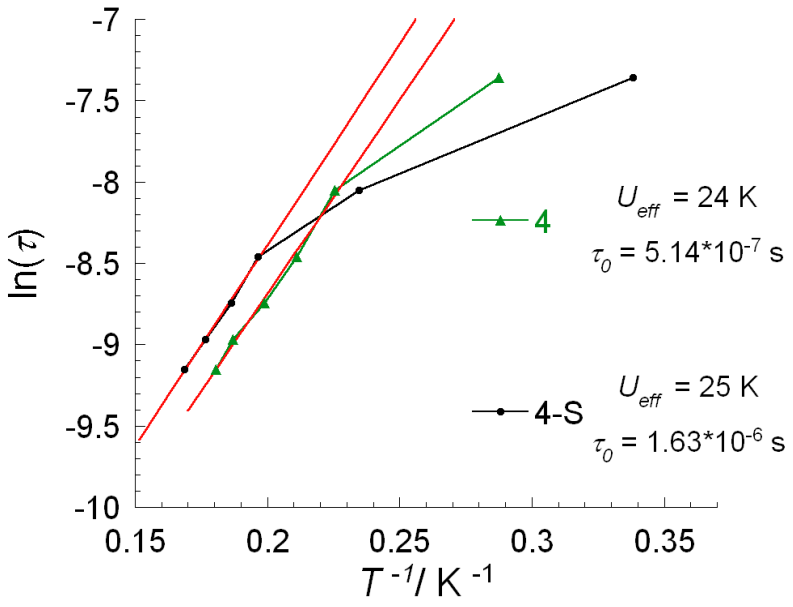

Figure S14. Relaxation time of the magnetization ln(τ) *vs*. T^{-1} (Arrhenius Plot using ac data) of 4 (triangle) and 4-S (circle). The solid red line corresponds to the fit.

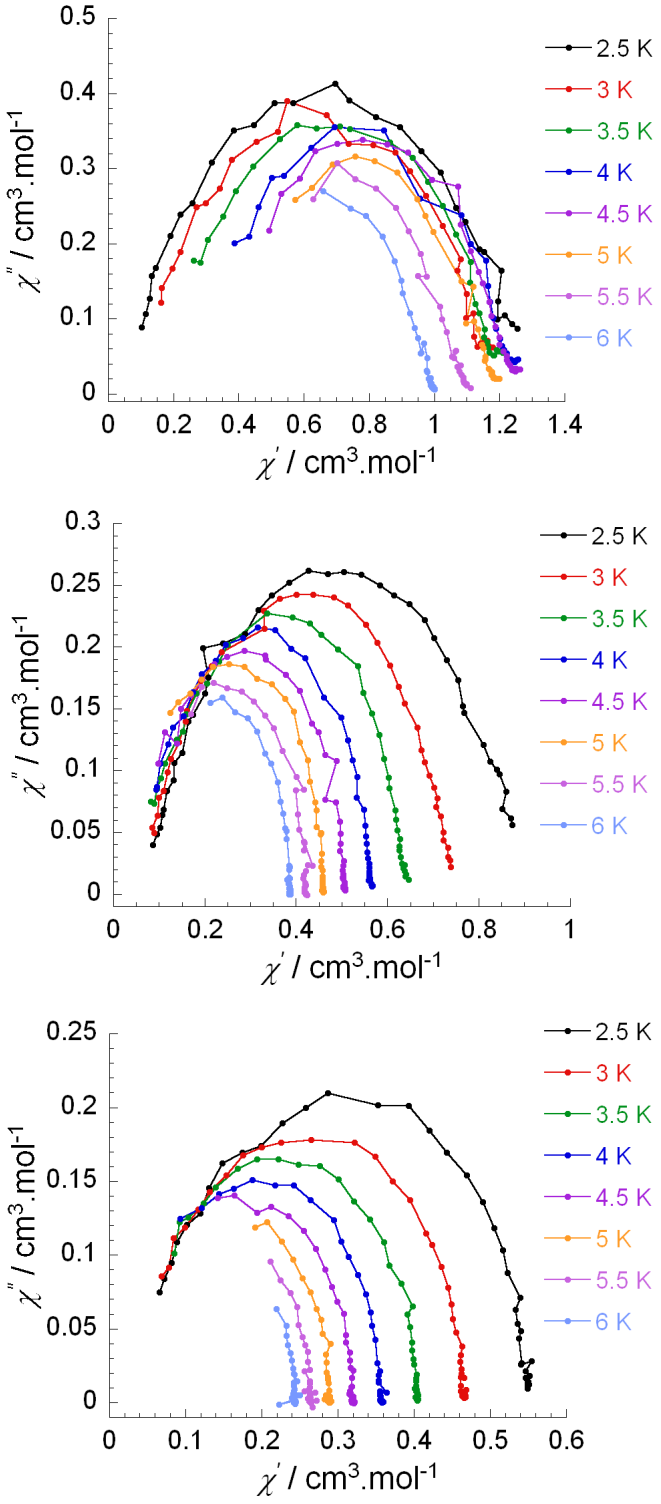

Figure S15. Cole-Cole plots for **3** (top), **4** (middle) and **4-s** (bottom)